European Journal of Medicinal Chemistry 44 (2009) 1415–1426

Contents lists available at ScienceDirect

European Journal of Medicinal Chemistry

journal homepage: http://www.elsevier.com/locate/ejmech

Original article

^{11}C-labelled PIB analogues as potential tracer agents for in vivo imaging of amyloid β in Alzheimer's disease

K. Serdons [a,*], T. Verduyckt [a], D. Vanderghinste [a], P. Borghgraef [b], J. Cleynhens [a], F. Van Leuven [b], H. Kung [c], G. Bormans [a], A. Verbruggen [a]

[a] Laboratory for Radiopharmacy, Faculty of Pharmaceutical Sciences, K.U. Leuven, O&N2, Herestraat 49 – Bus 821, 3000 Leuven, Belgium
[b] Laboratory of Experimental Genetics and Transgenesis, K.U. Leuven, O&N1, Herestraat 49 – Bus 602, 3000 Leuven, Belgium
[c] Department of Radiology, University of Pennsylvania, Market Street 3700 – Room 305, Philadelphia, United States

ARTICLE INFO

Article history:
Received 8 May 2008
Received in revised form 18 September 2008
Accepted 18 September 2008
Available online 7 October 2008

Keywords:
Alzheimer's disease
Amyloid
Diagnosis
PET
Carbon-11
PIB
Phenylbenzothiazole

ABSTRACT

Pittsburgh Compound-B (PIB) is currently being evaluated clinically for in vivo visualization of amyloid plaques in patients with Alzheimer's disease (AD). We have synthesized three structural isomers of 6-hydroxy-2-(4′-aminophenyl)-1,3-benzothiazole, performed radiolabelling with carbon-11 and investigated their in vivo and in vitro properties. Specific binding to amyloid plaques was demonstrated in vitro using post-mortem brain homogenates of AD patients, transgenic AD mice brain sections and post-mortem human AD brain sections. In normal mice, initial brain uptake (at 2 min p.i.) was high and was followed by a fast wash-out. The three structural analogues have a high potential as tracer agents for in vivo visualization of amyloid plaques in AD patients.

1. Introduction

The increasing mean life span of the global population emphasizes the need for accurate diagnostic tools and therapies for age-related diseases such as Alzheimer's disease (AD) which has an exponentially increasing incidence with age [1]. Alzheimer's disease is the most frequent form of dementia and is characterized by a progressive neurodegeneration. The hallmarks of AD are an extracellular deposition of amyloid β (Aβ) in the form of neuritic plaques, an intraneuronal cytoplasmatic deposition of neurofibrillary tangles (NFTs), activated microglia and reactive astrocytes [2]. Although scientists are uncovering more and more of the pathogenesis of AD, it is still not entirely clear what the exact correlation is between the neuritic plaques and the NFTs [3–5]. Nevertheless, the amyloid cascade hypothesis presented by Hardy and Higgins in 1991 [6] is still up-to-date and highlights the importance of Aβ deposits and NFTs as potential targets for therapies against AD and as diagnostic tracer agents.

Until now, post-mortem histological staining of amyloid plaques with specific dyes (silver staining, Congo red, thioflavin-S, thioflavin-T (ThT),…) or using amyloid β antibodies is the only way to obtain a definitive diagnosis of AD. To allow non-invasive in vivo diagnosis of AD, the search for a radiolabelled derivative of one of these dyes has become subject of worldwide research. There are, however, a number of challenges to reach this goal. First of all, the tracer agent has to be able to cross the blood-brain barrier (BBB). This requires a neutral molecule with a molecular mass not exceeding 600 [7]. Furthermore, the log octanol-buffer partition coefficient (log *P*), which is a measure of the lipophilicity of the compound, should be preferably between 1 and 2.5 [8]. The ability to pass the BBB has to be combined with a high affinity for amyloid β plaques and the compound must be radiolabelled with a suitable radionuclide to allow detection of the radiation emitted by the

Abbreviations: AD, Alzheimer's disease; Aβ, amyloid β; APP, amyloid precursor protein; BBB, blood-brain barrier; ESI, electrospray ionization; FCS, fetal calf serum; ID, injected dose; IMPY, 6-iodo-2-(4′-dimethylamino)phenyl-imidazo[1,2]pyridine; LC–MS, liquid chromatography hyphenated to mass spectrometry; Mp, melting point; MPLC, medium pressure liquid chromatography; NFT, neurofibrillary tangle; NMP, *N*-methyl-2-pyrrolidone; NMR, nuclear magnetic resonance; *P*, partition coefficient; PBS, phosphate buffered saline; PBST, PBS containing 0.05% Tween® 20; PET, positron emission tomography; PIB, Pittsburgh Compound-B, 6-hydroxy-2-(4′-*N*-[^{11}C]methylaminophenyl)-1,3-benzothiazole; PPA, polyphosphoric acid; RP-HPLC, reversed phase high performance liquid chromatography; RT, room temperature; ThT, thioflavin-T; TLC, thin layer chromatography.

* Corresponding author. Tel.: +3216330441; fax: +3216330449.
E-mail address: kim.serdons@pharm.kuleuven.be (K. Serdons).

0223-5234/$ – see front matter © 2008 Elsevier Masson SAS. All rights reserved.
doi:10.1016/j.ejmech.2008.09.038

tracer agent outside the patient's body using a gamma or positron emission tomography (PET) camera ultimately providing quantitative in vivo images of amyloid β plaque deposition in the brain.

In the past years, radiolabelled derivatives of several of the higher mentioned dyes have been tested and reported [9–18]. Up to now, by far the most promising and clinically useful results have been obtained with [^{11}C]PIB (6-hydroxy-2-(4′-N-[^{11}C]methylaminophenyl)-1,3-benzothiazole, Fig. 1), but early clinical evaluation of fluorine-18 labelled derivatives is also ongoing [12,19]. In a search for derivatives with improved characteristics we synthesized and labelled in the present study three structure analogues of this compound, namely the 4-hydroxy, 5-hydroxy and 7-hydroxy structural isomers (Fig. 1). We compared their in vivo and in vitro biological characteristics with those of the parent compound [^{11}C]PIB to obtain structure activity information related to the position of the OH-group which would also be relevant for the development of new ^{18}F-labelled PIB derivatives.

2. Results and discussion

2.1. Synthesis

2.1.1. Synthesis of 4-hydroxy-, 5-hydroxy- and 7-hydroxy-2-(4′-aminophenyl)-1,3-benzothiazole (**5a**–**c**)

The three compounds were synthesized using a similar pathway (Scheme 1) [20]. For the synthesis of 4-hydroxy-2-(4′-aminophenyl)-1,3-benzothiazole (**5a**), ring closure of the benzothiazole does not yield two isomers and further separation was not required. Briefly, *o*-anisidine was first reacted with *p*-nitrobenzoyl chloride to form *N*-2′-methoxyphenyl-4-nitrobenzamide (**1a**). The amide was then converted to the thiobenzamide (**2a**) using Lawesson's reagent (2,4-bis(4-methoxyphenyl)-1,3-dithia-2,4-diphosphetane-2,4-disulphide) which is a useful thiation reagent to replace the carbonyl oxygen atoms of ketones, amides and esters by sulphur. In the presence of potassium ferricyanide, **2a** was cyclized to the 2-(4′-nitrophenyl)-benzothiazole **3a**. After reduction of the nitro to an amine group using $SnCl_2$, the methyl ether was demethylated using boron tribromide (BBr_3) in dichloromethane at 70 °C, yielding **5a**. For the synthesis of 5-hydroxy-2-(4′-aminophenyl)-1,3-benzothiazole (**5b**) and 7-hydroxy-2-(4′-aminophenyl)-1,3-benzothiazole (**5c**), ring closure can lead to the formation of two isomers and therefore the procedure described by Hutchinson [21] was used. When a halogen atom (typically chlorine or bromine) is present in the position where the ring closure should occur and sodium hydride (NaH) or sodium methoxide (NaOMe) is used in combination with *N*-methyl-2-pyrrolidone (NMP) as a solvent, the ring closure is specific for the intended position. Using this procedure, we were able to obtain **5b** and **5c** in sufficient yield. For the synthesis of 7-hydroxy-2-(4′-aminophenyl)-1,3-benzothiazole (**5c**) the starting compound 2-bromo-3-aminoanisole was obtained following a reported procedure [22]. However, for the synthesis of **5b**, the commercially available hydrochloride salt of 6-chloro-*m*-anisidine was used as starting product resulting in a much higher overall yield.

2.1.2. Synthesis of 4-hydroxy-2-(4′-methylaminophenyl)-1,3-benzothiazole (**6a**) and 7-hydroxy-2-(4′-methylaminophenyl)-1,3-benzothiazole (**6c**)

A small amount of **6a** and **6c** was synthesized by methylation of **5a** and **5c**, respectively, using iodomethane (Scheme 2). Mass spectrometric analysis of the reaction mixture showed the presence of both the *N*-dimethylated and *N*-monomethylated **6**. Reversed phase high performance liquid chromatography (RP-HPLC) analysis further showed that the obtained monomethylated compound had a longer retention time than the methoxy-isomer (**4**), indicating that methylation had occurred at the amino group. *O*-methylation normally requires deprotonation of the phenol and thus requires more alkaline reaction conditions. Purification was done using medium pressure liquid chromatography (MPLC).

2.1.3. Synthesis of 5-hydroxy-2-(4′-methylaminophenyl)-1,3-benzothiazole (**6b**)

To avoid a difficult MPLC separation of the mono- and dimethylamino derivative resulting from the methylation reaction, **6b** was prepared using the method described by Lin (Scheme 3) [23]. The benzothiazole ring of commercially available 5-methoxy-2-methyl-benzothiazole was opened using 10 M sodium hydroxide in order to obtain 2-amino-4-methoxy-thiophenol (**7**), which then was reacted with 4-(methylamino)benzoic acid in polyphosphoric acid (PPA) to obtain **8** after further purification using column chromatography. The methoxy group was then converted to a hydroxy group using BBr_3 to obtain **6b** in a 69% yield.

2.2. Radiolabelling

2.2.1. Synthesis of 4-hydroxy-2-(4′-[^{11}C]methylaminophenyl)-1,3-benzothiazole ([^{11}C]**6a**), 5-hydroxy-2-(4′-[^{11}C]methylaminophenyl)-1,3-benzothiazole ([^{11}C]**6b**) and 7-hydroxy-2-(4′-[^{11}C]methylaminophenyl)-1,3-benzothiazole ([^{11}C]**6c**)

^{11}C-methylation of precursor **5a** was performed with a 25% yield by bubbling [^{11}C]$CH_3OSO_2CF_3$ (methyltriflate) with a stream of helium through a solution of the precursor (Scheme 4). Pre-purification of the reaction mixture was done with the aid of an activated C-18 Sep-Pak® cartridge, which retained [^{11}C]**6a** whereas more hydrophilic compounds (such as [^{11}C]methyltriflate) were eluted from the cartridge. After rinsing the cartridge with water, the labelled compound [^{11}C]**6a** was eluted with methanol. The eluate containing [^{11}C]**6a** was further purified by RP-HPLC on a semi-preparative C18 column. The use of a semi-preparative column was necessary to allow injection of the entire prepurified reaction mixture. During isolation of the desired ^{11}C-labelled benzothiazole care was taken to start the collection of the peak only after the UV-signal had returned to baseline, in order to prevent contamination of the carbon-11 labelled benzothiazole with the non-radioactive precursor. Identity confirmation was done using radio-HPLC combined with mass spectrometry (radio-LC–MS) (experimental mass: 257 Da, theoretical mass: 257 Da in ES^+, data not shown) and by comparison of the retention times of the authentic analogue **6a** and the ^{11}C-labelled [^{11}C]**6a** on RP-HPLC. Starting from **5b** and **5c**,

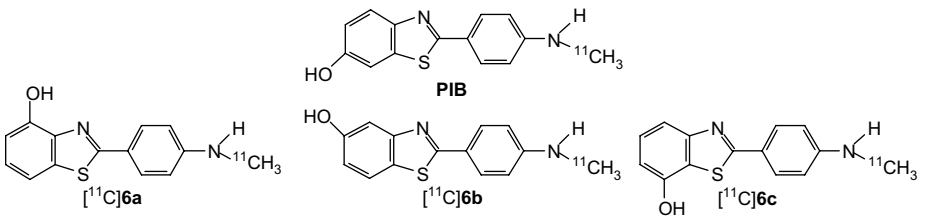

Fig. 1. Structure of PIB, 4-hydroxy-2-(4′-[^{11}C]methylaminophenyl)-1,3-benzothiazole [^{11}C]**6a**, 5-hydroxy-2-(4′-[^{11}C]methylaminophenyl)-1,3-benzothiazole [^{11}C]**6b** and 7-hydroxy-2-(4′-[^{11}C]methylaminophenyl)-1,3-benzothiazole [^{11}C]**6c**.

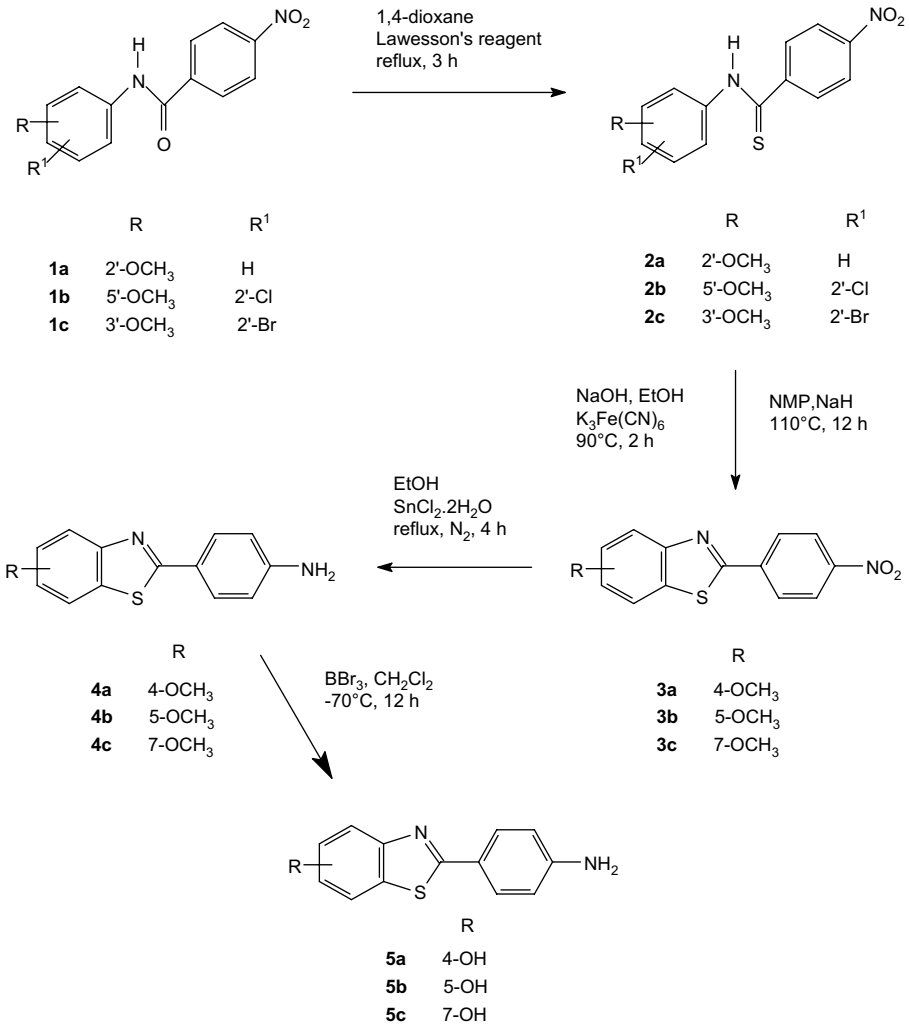

Scheme 1. Synthesis of 4-hydroxy-2-(4′-aminophenyl)-1,3-benzothiazole (**5a**), 5-hydroxy-2-(4′-aminophenyl)-1,3-benzothiazole (**5b**) and 7-hydroxy-2-(4′-aminophenyl)-1,3-benzothiazole (**5c**).

the same procedure as for [^{11}C]**6a** was followed to prepare [^{11}C]**6b** and [^{11}C]**6c**, respectively. Despite the low labelling yield of 5% and 7%, respectively (not decay corrected), sufficient quantities of the ^{11}C-labelled tracer were obtained to perform the biological studies and no attempts were made to increase the labelling yield.

2.3. Partition coefficient

The log *P* values of [^{11}C]**6a**, [^{11}C]**6b** and [^{11}C]**6c** were found to be 3.18 ± 0.18, 2.48 ± 0.063 and 2.45 ± 0.096, respectively. The difference in log *P* values of [^{11}C]**6a** on the one hand and [^{11}C]**6b** and [^{11}C]**6c** on the other hand can be explained by an assumed formation of an intramolecular hydrogen bond in compound [^{11}C]**6a** (Fig. 2), making the compound more lipophilic. Indeed, if no intramolecular hydrogen bond formation is possible, the lipophilicity of the 4-hydroxy derivative on the one hand and the 5-hydroxy and 7-hydroxy derivatives on the other hand is approximately the same, as demonstrated by an identical retention time of 4-methoxy-2-(4′-aminophenyl)-1,3-benzothiazole and 6-methoxy-2-(4′-aminophenyl)-1,3-benzothiazole using RP-HPLC (data not shown).

2.4. Affinity of the authentic non-radiolabelled derivatives *6a*, *6b* and *6c* for post-mortem human AD brain homogenates

In order to obtain information on the in vitro affinity of these tracers for amyloid β fibrils, determination of their binding to human AD brain homogenates is a useful test. The K_i values

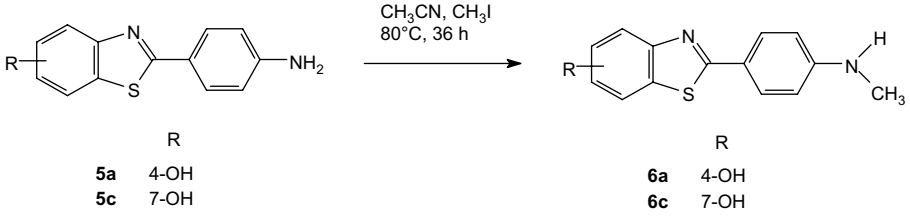

Scheme 2. Synthesis of 4-hydroxy-2-(4′-methylaminophenyl)-1,3-benzothiazole (**6a**) and 7-hydroxy-2-(4′-methylaminophenyl)-1,3-benzothiazole (**6c**).

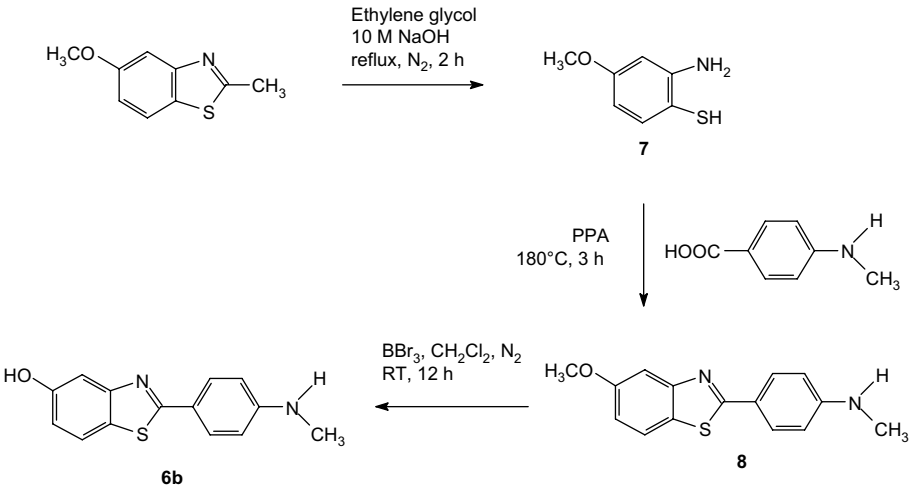

Scheme 3. Synthesis of 5-hydroxy-2-(4′-methylaminophenyl)-1,3-benzothiazole (**6b**).

obtained for the authentic non-radioactive compounds are given in Table 1. Compounds with a low K_i value ($\leq$20 nM) show good affinity for Aβ plaques. Pittsburgh Compound-B showed a K_i value of 2.8 ± 0.5 nM in this test, indicating that the new compounds have a similar affinity for amyloid β as PIB.

2.5. Binding of **6a**, **6b** and **6c** to amyloid plaques in mouse and human AD brain sections

The potential of binding to amyloid β plaques of compounds **6a**, **6b** and **6c** was also evaluated in post-mortem brain sections of transgenic AD mice and in post-mortem brain sections of an AD patient. Both 40-μm vibratome sections and 8-μm paraffin sections of brain can be used for this purpose. Vibratome sections normally are incubated with the non-radioactive compound in free floating conditions, maximizing the contact surface between the solution and the brain section. Paraffin sections benefit from the fact that they are thinner than vibratome sections. Here they were used for performing 'co-localization' experiments. In such experiments, a section is incubated with one of the non-radioactive reference compounds, which can be visualized with fluorescence microscopy as the bound benzothiazole is fluorescent, while an adjacent serial section can be stained immunohistochemically with the AβN25 or pan Aβ antibody that binds to fibrillar amyloid β. If the non-radioactive compound binds to fibrillar amyloid β on a particular section, the localization of the fluorescence on this section has to be almost identical to the localization of the antibody on the adjacent section. Such a co-localization experiment is almost impossible to perform with vibratome sections since such sections are 40 μm thick whereas the typical diameter of an amyloid plaque is 100 μm. However, incubation of a vibratome section with the fluorescent compounds (**6a**, **6b** or **6c**) and the AβN25 (or pan Aβ) antibody simultaneously, also enables to obtain useful co-localization data. The results of the incubation of 8-μm microtome sections of transgenic AD mouse brain and post-mortem human AD brain with either **6a**, **6b** or **6c** at a 1-μM concentration and of the immunohistochemical staining of neighbouring sections is shown in Figs. 3 and 4. The region of the mouse brain shown is the subiculum, a structure rich in Aβ plaques in AD mice that is located in the hippocampal region. The region shown in the human brain is part of the cortex. From both figures it can be seen that **6a** as well as **6b** and **6c** stain plaques in transgenic AD mouse brain as well as in human AD brain. Comparable images were obtained using the PIB-compound (data not shown). This is in accordance with the findings from the in vitro affinity test. Comparison of the images of the immunohistochemical staining with the images obtained with fluorescence microscopy shows that the AβN25 and pan Aβ antibody stain more Aβ plaques than the benzothiazoles. This is a consequence of the much higher affinity of the AβN25 and pan Aβ antibody for amyloid β plaques in comparison to the affinity of **6a**, **6b** and **6c**. From Fig. 4 it also appears that the benzothiazoles primarily stain the core of the amyloid β plaque. To further evaluate this, a vibratome section was incubated first with the AβN25 antibody and then with **6b**. This co-localization is shown in Fig. 5. In these images, the outer rim of the plaque is only stained with the AβN25 antibody, which colors both the dense and diffuse parts of the plaque, while the core of the amyloid β plaque shows intensive fluorescence. This is probably a consequence of the higher amount of β-pleated sheets in the core of the plaque and proves the assumption that these benzothiazoles primarily label the core of the amyloid β plaque. Other vibratome sections from transgenic AD mouse brain also show that **6b** and **6c** can be used to visualize vascular amyloid as can be seen in Fig. 6. In these images the background signal is higher in the right section stained with **6c**

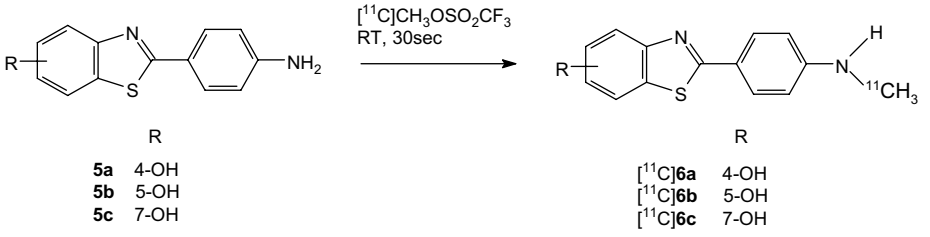

Scheme 4. Radiosynthesis of 4-hydroxy-2-(4′-[^{11}C]methylaminophenyl)-1,3-benzothiazole ([^{11}C]**6a**), 5-hydroxy-2-(4′-[^{11}C]methylaminophenyl)-1,3-benzothiazole ([^{11}C]**6b**) and 7-hydroxy-2-(4′-[^{11}C]methylaminophenyl)-1,3-benzothiazole ([^{11}C]**6c**).

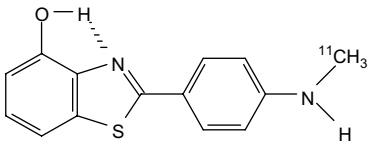

Fig. 2. Formation of an intramolecular hydrogen bond in compound [^{11}C]**6a**.

than in the left section stained with **6b**. Both compounds highlight the presence of vascular amyloid, but the fluorescent signal with **6b** is more intense than that of **6c**. Therefore, the test was repeated using a 0.1 μM concentration of the compounds (data not shown). As could be expected from Fig. 6, this lower concentration still yielded useful fluorescence images with **6b** with a lower background signal, while the fluorescence signal was close to the detection limit for **6c**. The three compounds stain amyloid plaques in human AD brain as well as in transgenic AD mouse brain. Compound **6a** not only binds to the plaques, but also to neurofibrillary tangles (Fig. 7). This behaviour has also been observed with other compounds, such as the ^{18}F-labelled FDDNP and BF-108 [12,18,24]. The reason, according to Suemoto et al. [18], is that plaques and neurofibrillary tangles share the β-sheet secondary structure.

Both in vitro tests show promising results for the ^{11}C-labelled PIB analogues. After intravenous injection of tracer amounts of the ^{11}C-labelled molecules it can be expected that specific binding will only occur at high affinity binding sites in the amyloid β plaques. However, for most of the reported amyloid PET tracers, a substantial fraction of the tracer also shows non-specific binding to white matter, decreasing both the image contrast and amyloid detection sensitivity. Determination of the in vitro affinity using amyloid containing human brain homogenate yields quantifiable affinity constant values whereas the clearance of non-specifically bound tracer is difficult to predict in vitro. High resolution fluorescence microscopy can be used to determine whether binding of the studied compounds is limited to amyloid binding sites, but this technique uses micromolar amounts of the non-radioactive counterparts instead of the nanomolar tracer amounts used in vivo. At micromolar concentration also lower affinity binding sites may be labelled and furthermore fluorescence intensity may depend on the target that the studied compound is binding to so that fluorescence images provide qualitative information rather than quantitative information.

Table 1
K_i values of **6a**, **6b** and **6c** competing with ^{125}I-IMPY binding to amyloid plaques in human AD brain homogenates.

Compound	K_i[a] (nM, mean ± SEM)
6a	18.8 ± 3.8
6b	11.5 ± 3
6c	11.2 ± 5
PIB	2.8 ± 0.5

[a] $K_i = IC_{50}/(1 + L/K_d)$ with IC_{50} = inhibition constant 50%, L = concentration radioactive ligand and K_d = dissociation constant of the radioactive ligand.

2.6. Biodistribution in healthy mice

Biodistribution of the three new tracer agents and PIB was studied in normal mice. Tables 2–5 list the tracer uptake in the most important organs. The initial brain uptake (2 min p.i.) of the three new compounds is in the same range as that of PIB. The initial uptake is slightly lower for the 7-hydroxy derivative [^{11}C]**6c** and slightly higher for the 5-hydroxy derivative [^{11}C]**6b**. The 5-hydroxy and 7-hydroxy derivatives [^{11}C]**6b** and [^{11}C]**6c**, respectively, show equal initial uptake in cerebrum and cerebellum (expressed as % ID/g). The 4-hydroxy derivative [^{11}C]**6a** shows a higher activity concentration in the cerebrum compared with the cerebellum, which is also the case for PIB. With respect to brain wash-out (% ID in cerebrum at 2 min/% ID in cerebrum at 60 min), the 4-hydroxy and 7-hydroxy derivatives [^{11}C]**6a** and [^{11}C]**6c**, respectively, show a wash-out which is 2 times faster than that of PIB. The 5-hydroxy derivative [^{11}C]**6b** even has a brain wash-out that is 8 times faster

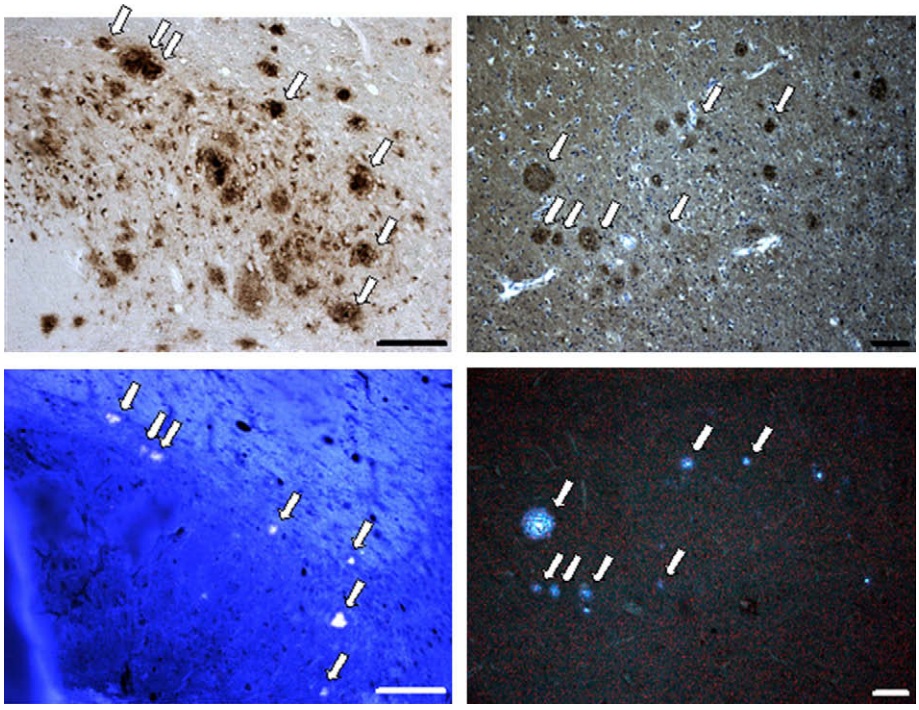

Fig. 3. Immunohistochemical and fluorescent staining of 8-μm microtome sections of transgenic mouse brain (left) and post-mortem human AD brain (right). Top images are of sections immunohistochemically stained with pan Aβ antibody, the bottom images are of sections incubated with **6a** and investigated with fluorescence microscopy. Bar = 100 μm.

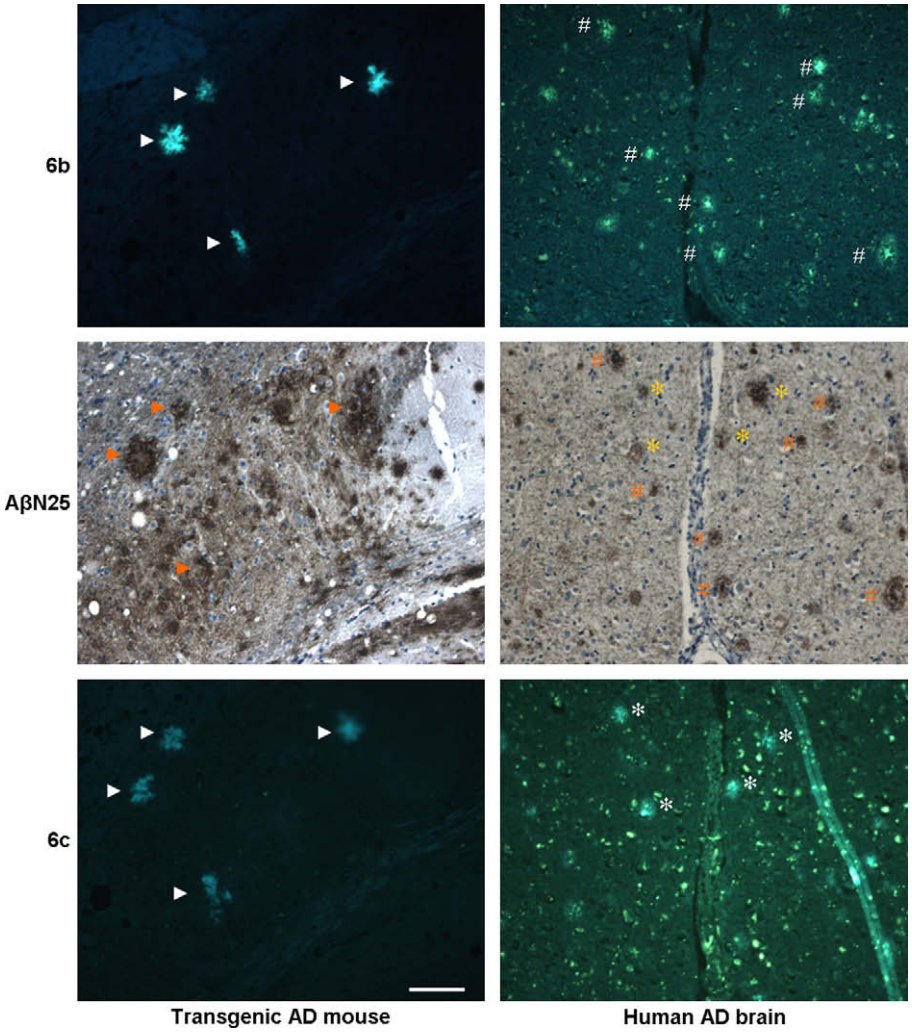

Fig. 4. Fluorescence microscopic images after incubation of transgenic AD mouse brain (left) and human AD brain (right) with **6b** (top) or **6c** (bottom). Middle row is immunohistochemically stained with AβN25. Bar = 100 μm. From top to bottom are three serial sections. Amyloid β plaques in AD mouse brain highlighted with white arrowheads (top/bottom) or red arrowheads (middle). Amyloid β plaques in human AD brain marked with # for **6b** (corresponding plaques immunohistochemically stained marked with red #) or with * for **6c** (corresponding plaques immunohistochemically stained marked with yellow *). (For interpretation of the references to color in this figure legend, the reader is referred to the web version of this article.)

than that of PIB over the studied time interval. In healthy mice, a compound with favourable characteristics for plaque imaging should show a high initial uptake followed by a rapid wash-out, thus without non-specific binding to any brain structure devoid of amyloid plaques. In view of these requirements, the 5-hydroxy derivative [^{11}C]**6b**, with its high initial brain uptake and very fast wash-out seems to be the most suitable tracer agent for in vivo diagnosis of AD, based on the mouse data. The distribution of these

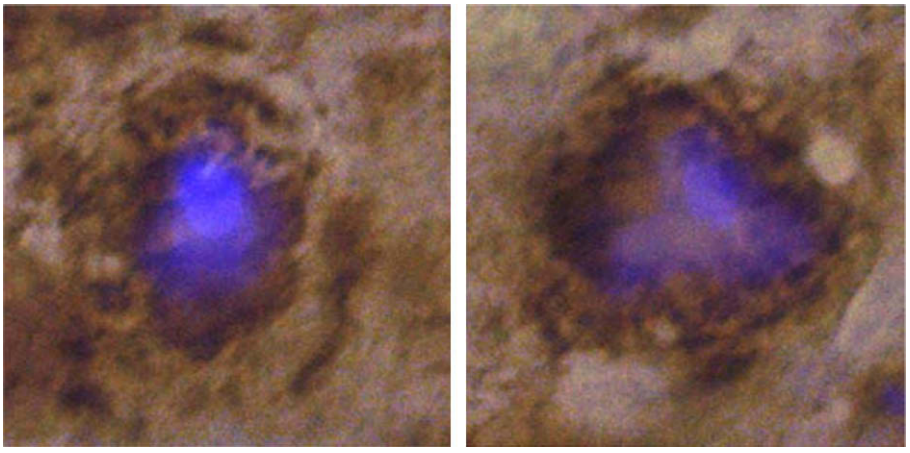

Fig. 5. Section of a vibratome section of a transgenic AD mouse brain stained with AβN25 (brown) in combination with **6b** (blue). Depicted are two enlarged plaques from an entire section. (For interpretation of the references to color in this figure legend, the reader is referred to the web version of this article.)

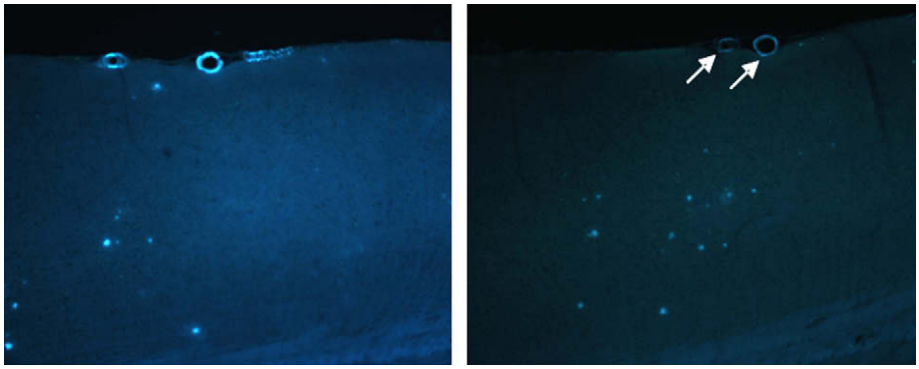

Fig. 6. Fluorescence microscopic images of vibratome sections of transgenic AD mouse brain cortex stained with a 1 μM solution of **6b** (left) or **6c** (right). Arrows indicate vascular amyloid.

tracer agents in other organs is of a lesser concern, except for the clearance of the activity from blood, which should be rapid in order to increase the target-to-non-target activity ratio. For the three new ^{11}C-labelled phenylbenzothiazoles, the clearance of the activity from blood (% ID/g blood at 2 min/% ID/g blood at 60 min) is relatively fast, ranging from 6 for the 4-hydroxy derivative [^{11}C]**6a** to 12 for the 7-hydroxy derivative [^{11}C]**6c** as compared to 3 for PIB, and is in the same range as the brain wash-out.

The studied ^{11}C-labelled phenylbenzothiazoles also show a moderate uptake in the kidneys and excretion in the urine. The total activity in the renal system (kidneys + urine) at 60 min p.i. varies from 15% ID for the 5-hydroxy derivative [^{11}C]**6b** to almost 30% ID for the 7-hydroxy derivative [^{11}C]**6c**. No correlation could be found between the lipophilicity of these compounds (log *P*) and their degree of renal handling. The hepatobiliar excretion to the intestines is also rather fast. The total activity in the hepatobiliary system at 60 min p.i. varies from about 59% of ID for the 4-hydroxy derivative [^{11}C]**6a** to 78% for the 5-hydroxy derivative [^{11}C]**6b**, which also showed the fastest blood clearance. This illustrates the effect of small structural differences on the biological behaviour of this type of compounds. Furthermore, the log *P* values of the 5- and 7-hydroxy derivatives [^{11}C]**6b** and [^{11}C]**6c**, respectively, are almost identical, while their biological behaviour is diverging. Although the log *P* value of the 4-hydroxy analogue [^{11}C]**6a** is higher, its in vivo values for initial brain uptake, hepatobiliary clearance and urinary clearance always are in between the values of the other two new compounds.

3. Conclusion

Three structural isomers of 6-hydroxy-2-(4′-aminophenyl)-1,3-benzothiazole have been synthesized and radiolabelled with a ^{11}C-labelled methyl group. We studied the biological characteristics of the new tracer agents with a focus on their potential use as PET probes for in vivo visualization of amyloid β. The log *P* values of 5-hydroxy-2-(4′-[^{11}C]methylamino)-1,3-phenylbenzothiazole [^{11}C]**6b**

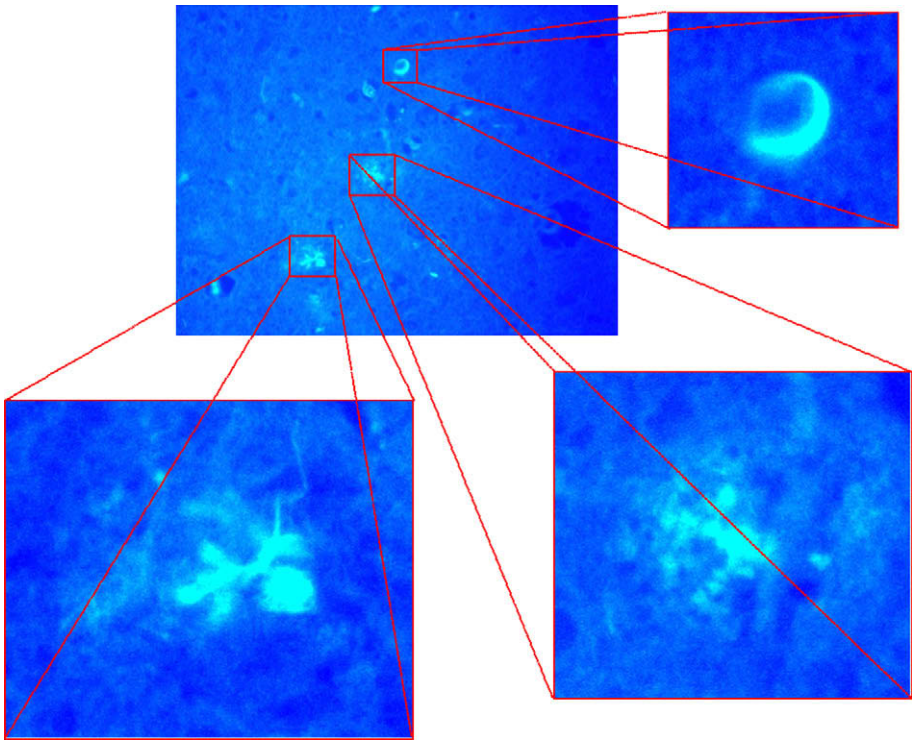

Fig. 7. Fluorescence microscopic images after incubation of 8-μm sections of post-mortem human AD brain with **6a**. The top left image shows an overview of the stained section. The top right image is a magnification of a section of the top left picture, showing a NFT. The bottom images are magnifications of plaques.

Table 2
Tissue distribution of 4-hydroxy-2-(4′-[^{11}C]methylaminophenyl)-1,3-benzothiazole [^{11}C]**6a** after i.v. injection in normal mice at 2 and 60 min p.i. ($n = 4$ at each time point).

	% ID ± s.d.		% ID/g tissue ± s.d.	
	2 min p.i.	60 min p.i.	2 min p.i.	60 min p.i.
Urine	0.2 ± 0.2	22.7 ± 6.3	–	–
Kidneys	10.6 ± 3.6	0.6 ± 0.2	19.4 ± 6.3	1.2 ± 0.4
Liver	21.2 ± 4.1	6.4 ± 2.4	11.1 ± 2.4	3.7 ± 1.5
Intestines	12.0 ± 1.0	52.3 ± 4.6	–	–
Cerebrum	1.2 ± 0.3	0.1 ± 0.1	3.8 ± 0.9	0.3 ± 0.3
Cerebellum	0.2 ± 0.1	0.0 ± 0.0	2.7 ± 2.1	0.6 ± 0.4
Blood	13.8 ± 1.0	2.3 ± 0.9	6.5 ± 0.5	1.0 ± 0.4

Table 4
Tissue distribution of 7-hydroxy-2-(4′-[^{11}C]methylaminophenyl)-1,3-benzothiazole [^{11}C]**6c** after i.v. injection in normal mice at 2 and 60 min p.i. ($n = 4$ at each time point).

	% ID ± s.d.		% ID/g tissue ± s.d.	
	2 min p.i.	60 min p.i.	2 min p.i.	60 min p.i.
Urine	0.58 ± 1.1	24.8 ± 2.9	–	–
Kidneys	9.0 ± 2.6	2.5 ± 0.98	16.9 ± 4.0	4.8 ± 1.8
Liver	27.8 ± 2.4	7.1 ± 0.59	14.5 ± 2.0	4.0 ± 0.38
Intestines	9.4 ± 2.2	54.7 ± 2.8	–	–
Cerebrum	0.83 ± 0.23	0.05 ± 0.01	2.6 ± 0.76	0.16 ± 0.03
Cerebellum	0.22 ± 0.05	0.01 ± 0.01	2.8 ± 0.49	0.10 ± 0.14
Blood	9.8 ± 0.78	1.2 ± 0.17	4.6 ± 0.40	0.57 ± 0.08

and 7-hydroxy-2-(4′-[^{11}C]methylamino)-1,3-phenylbenzothiazole [^{11}C]**6c** are similar to the value obtained for PIB, whereas that of the 4-hydroxy analogue [^{11}C]**6a** is significantly higher. The possibility of forming an intramolecular hydrogen bond is assumed to be the reason for this difference in log *P* value. The log *P* values of the 5- and 7-hydroxy analogues [^{11}C]**6b** and [^{11}C]**6c**, respectively, are in good range for passive diffusion over the BBB, while the log *P* value of the 4-hydroxy compound [^{11}C]**6a** is rather high, which might lead to residual background activity in the brain because of non-specific binding to white matter. The affinity of the three structure isomers for amyloid β on the other hand is roughly the same. They all show suitable binding affinity for post-mortem human AD brain homogenates as well as affinity to sections of post-mortem transgenic AD mouse brain and human AD brain. The 5-hydroxy analogue [^{11}C]**6b** seems to have the most favourable in vivo pharmacokinetics in brain. It shows the highest brain uptake of the three isomers at 2 min p.i. and its brain wash-out within the 2-min to 60-min p.i. interval is 8 times faster than that of PIB. Accordingly, the 5-hydroxy analogue [^{11}C]**6b** shows a rapid blood clearance, 4 times faster than that of PIB. Significant differences have been observed in general biodistribution characteristics of the respective agents, not necessarily in line with their log *P* value. These differences indicate that very subtle structural modifications in this class of ThT-derivatives can have a significant influence on the in vivo behaviour. Overall, the results indicate that these analogues deserve further evaluation as potential useful tracer agents for in vivo visualization of amyloid plaques.

4. Experimental protocols

4.1. Materials and general procedures

All reagents and solvents used in synthesis were obtained from Acros Organics (Geel, Belgium), Aldrich, Fluka or Sigma (Sigma–Aldrich, Bornem, Belgium) and were used without further purification. $MgSO_4$ was used as drying agent. Evaporation of organic solvents under reduced pressure was done with a Büchi Rotovapor (Büchi, Flawil, Switzerland). Purification of the reaction mixtures was done by column chromatography using silica gel with a particle size varying between 0.04 and 0.063 mm (230–400 Mesh) (MN Kieselgel 60 M, Macherey-Nagel, Düren, Germany) as the stationary phase or by medium pressure liquid chromatography (MPLC). The MPLC-system consisted of a Büchi, model B-680 pump and a column (internal diameter 2.5 cm, length 45 cm) filled with octadecylsilyl silica gel (LiChroprep®, 15–25 μm, mean pore diameter 100 Å, Merck, Darmstadt, Germany). The column was eluted using mixtures of acetonitrile and 0.05 M ammonium acetate and the eluate was monitored for UV absorbance at 254 nm (Econo UV monitor model EM-1, Biorad, Hercules, CA). For thin layer chromatography (TLC) precoated silica TLC plates were used (DC-Alufolien-Kieselgel, Fluka, Buchs, Switzerland). The structure of the synthesized products was confirmed with ^{1}H nuclear magnetic resonance (NMR) spectroscopy on a Gemini 200 MHz spectrometer (Varian, Palo Alto, CA, USA). Chemical shifts are reported as δ-values (parts per million) relative to tetramethylsilane ($\delta = 0$). Coupling constants are reported in hertz. Splitting patterns are defined by s (singlet), d (doublet), dd (double doublet), t (triplet) and m (multiplet). Melting points (Mps) were determined with an IA9100 digital melting point apparatus (Electrothermal, Essex, UK) in open capillaries and are reported uncorrected.

Carbon-11 was produced by irradiation of N_2-gas (containing 1% O_2) with 10-MeV protons generated by a Cyclone 10/5 cyclotron (Ion Beam Applications, Louvain-La-Neuve, Belgium).

Quantitative determination of radioactivity in samples was done using an automatic gamma counter coupled to a multi-channel analyzer (Wallac 1480 Wizard® 3″, Wallac, Turku, Finland).

The reversed phase high performance liquid chromatography (RP-HPLC) system consisted of a Merck–Hitachi ternary gradient pump (model L-6200A intelligent pump, Merck) and an XTerra™ RP C18 column (5 μm, 250 mm × 4.6 mm) (Waters, Milford, MA, USA). The eluate was monitored for UV absorbance at 254 nm with a dual wavelength absorbance detector (Waters 2487) and for radioactivity with a 3-inch NaI(Tl) scintillation detector coupled to a single channel analyzer (ACEMate™ amplifier and bias supply, EG&G ORTEC). The mobile phase consisted of a mixture of acetonitrile and

Table 3
Tissue distribution of 5-hydroxy-2-(4′-[^{11}C]methylaminophenyl)-1,3-benzothiazole [^{11}C]**6b** after i.v. injection in normal mice at 2 and 60 min p.i. ($n = 4$ at each time point).

	% ID ± s.d.		% ID/g tissue ± s.d.	
	2 min p.i.	60 min p.i.	2 min p.i.	60 min p.i.
Urine	0.35 ± 0.23	14.6 ± 2.2	–	–
Kidneys	8.1 ± 1.5	0.70 ± 0.70	14.2 ± 1.8	1.2 ± 1.2
Liver	25.8 ± 2.4	4.2 ± 1.5	12.1 ± 1.7	2.2 ± 0.91
Intestines	12.9 ± 2.7	73.7 ± 3.3	–	–
Cerebrum	1.3 ± 0.25	0.03 ± 0.00	4.3 ± 0.45	0.09 ± 0.02
Cerebellum	0.57 ± 0.08	0.01 ± 0.00	4.4 ± 0.54	0.08 ± 0.07
Blood	6.0 ± 0.70	0.50 ± 0.06	2.5 ± 0.30	0.21 ± 0.03

Table 5
Tissue distribution of 6-hydroxy-2-(4′- [^{11}C]methylaminophenyl)-1,3-benzothiazole or [^{11}C]PIB after i.v. injection in normal mice at 2 and 60 min p.i. ($n = 4$ at each time point).

	% ID ± s.d.		% ID/g tissue ± s.d.	
	2 min p.i.	60 min p.i.	2 min p.i.	60 min p.i.
Urine	0.2 ± 0.1	24.4 ± 10.1	–	–
Kidneys	10.3 ± 3.8	4.8 ± 3.9	19.9 ± 9.1	9.1 ± 7.1
Liver	15.6 ± 4.5	9.8 ± 2.6	7.9 ± 2.6	5.0 ± 1.7
Intestines	12.0 ± 2.4	42.5 ± 7.5	–	–
Cerebrum	1.1 ± 0.4	0.2 ± 0.1	3.6 ± 1.4	0.6 ± 0.2
Cerebellum	0.2 ± 0.0	0.0 ± 0.0	1.6 ± 0.1	0.3 ± 0.1
Blood	7.9 ± 0.5	2.7 ± 0.8	3.1 ± 0.2	1.1 ± 0.3

0.05 M ammonium acetate (unless otherwise stated) and gradient as well as isocratic elution were used. Data were collected with a RaChel data acquisition system (Lablogic, Sheffield, UK).

Radio-HPLC combined with mass spectrometry (radio-LC-MS) was performed on a system consisting of a Waters Alliance 2690 separation module coupled to a reverse phase XTerra™ MS C18 3.5 μm column (2.1 mm × 50 mm) (Waters). The column eluate was monitored for UV absorbance (Waters 2487 Dual wavelength absorbance detector) and for radioactivity (3-inch NaI(Tl)-crystal coupled to a single channel analyzer (The Nucleus, Oak Ridge, TE, USA)) and then analyzed in a time-of-flight mass spectrometer (LCT, Micromass, Manchester, England) equipped with an electrospray ionization (ESI) source. Acquisition and processing of data were performed with Masslynx software (version 3.5).

Gas chromatography was performed with a DI 200 gas chromatograph (Delsi Instruments, Suresnes, France) with a Porapak QS 80/100 column (Alltech, Lokeren, Belgium) of 180 cm × 0.25 inch.

4.2. Synthesis

4.2.1. Synthesis of 4-hydroxy-2-(4′-aminophenyl)-1,3-benzothiazole (**5a**)

4.2.1.1. N-*2′-Methoxyphenyl-4-nitrobenzamide (**1a**), method A.* A solution of *o*-anisidine (24.63 g, 200 mmol) and *p*-nitrobenzoyl chloride (37.11 g, 200 mmol) in pyridine (250 ml) was heated under reflux for 2 h. After cooling to room temperature (RT), the resulting solution was poured into water. The precipitate was filtered off, washed with water and dried in a vacuum oven. Crystallization from methanol yielded 43 g of **1a** (158 mmol, 79%) under the form of light yellow flakes. ^{1}H NMR (DMSO-d_6, 200 MHz): δ 3.83 (3H, s, OC$\underline{H}_3$); δ 6.98 (1H, dd, $^3J = 7.5$ Hz, 4′-H); δ 7.01 (1H, d, $^3J = 8.4$ Hz, 3′-H); δ 7.22 (1H, dd, $^3J = 7.7$ Hz, 5′-H); δ 7.71 (1H, d, $^3J = 7.6$ Hz, 6′-H); δ 8.17 (2H, d, $^3J = 8.8$ Hz, 2-H 6-H); δ 8.34 (2H, d, $^3J = 7.6$ Hz, 3-H 5-H). Accurate MS ES$^-$ *m/z* $[M-H]^-$ 271.0705 (calculated for $C_{14}H_{11}N_2O_4$ 271.0724). Mp: 129–130 °C.

4.2.1.2. N-*2′-Methoxyphenyl-4-nitrothiobenzamide (**2a**), method B.* A solution of **1a** (40.84 g, 150 mmol) and Lawesson's reagent (40.04 g, 90 mmol) in 1,4-dioxane (350 ml) was heated under reflux for 3 h, after which it was cooled to RT and poured into water. The precipitate was filtered off, washed with water and dried in a vacuum oven. Purification was done using column chromatography with dichloromethane/hexane (50:50 v/v) as eluent. Compound **2a** was obtained as 34.6 g of a red powder (120 mmol, 80%). ^{1}H NMR (DMSO-d_6, 200 MHz): δ 3.82 (3H, s, OC$\underline{H}_3$); δ 7.03 (1H, dd, $^3J = 7.4$ Hz, 4′-H); δ 7.16 (1H, d, $^3J = 7.8$ Hz, 3′-H); δ 7.36 (1H, dd, $^3J = 7.4$ Hz, 5′-H); δ 7.52 (1H, d, $^3J = 7.4$ Hz, 6′-H); δ 8.04 (2H, d, $^3J = 8.4$ Hz, 2-H 6-H); δ 8.30 (2H, d, $^3J = 8.4$ Hz, 3-H 5-H). Accurate MS ES$^-$ *m/z* $[M-H]^-$ 287.0478 (calculated for $C_{14}H_{11}N_2O_3S$ 287.0496). Mp: 132.5–134 °C.

*4.2.1.3. 4-Methoxy-2-(4′-nitrophenyl)-1,3-benzothiazole (**3a**).* A solution of **2a** (28.83 g, 100 mmol) in a mixture of ethanol (50 ml) and 10% (m/v) sodium hydroxide (300 ml) was slowly added over a period of 2 h to a solution of potassium ferricyanide (131.73 g, 400 mmol) in water (400 ml) at 90 °C. The obtained suspension was stirred for 2 h at 90 °C and then cooled to 4 °C. The precipitate was filtered off, washed with water and dried in a vacuum oven. The dry residue was dispersed in a mixture of dichloromethane/ethanol (75:25 v/v). The dispersion was filtered off and the filtrate was concentrated by vacuum evaporation. Purification was done by recrystallization from methanol/chloroform (75:25 v/v) to yield 13.7 g of **3a** as yellow needles (48 mmol, 48%). ^{1}H NMR ($CDCl_3$, 200 MHz): δ 4.11 (3H, s, OC$\underline{H}_3$); δ 6.97 (1H, d, $^3J = 7.9$ Hz, 5-H); δ 7.41 (1H, dd, $^3J = 8.1$ Hz, 6-H); δ 7.52 (1H, d, $^3J = 8.0$ Hz, 7-H); δ 8.29 (2H, d, $^3J = 5.6$ Hz, 2′-H 6′-H); δ 8.31 (2H, d, $^3J = 9.6$ Hz, 3′-H 5′-H). Accurate MS ES$^+$ *m/z* $[M+H]^+$ 287.0493 (calculated for $C_{14}H_{10}N_2O_3S$ 287.0485). Mp: 208.5–210.5 °C.

*4.2.1.4. 4-Methoxy-2-(4′-aminophenyl)-1,3-benzothiazole (**4a**), method C.* A dispersion of **3a** (10.02 g, 35 mmol) and stannous chloride dihydrate (23.7 g, 105 mmol) in ethanol (400 ml) was refluxed under nitrogen for 4 h. After cooling to RT, ethanol was removed by vacuum evaporation. The residue was dissolved in ethyl acetate (1500 ml) and the organic layer was washed with 2 M sodium hydroxide (500 ml), water (2 × 250 ml) and brine (250 ml). After drying with $MgSO_4$, the solvent was removed by vacuum evaporation. Purification was done using column chromatography with dichloromethane as eluent. Finally, 5.5 g of **4a** was obtained as a yellow powder (21 mmol, 60%). ^{1}H NMR ($CDCl_3$, 200 MHz): δ 4.05 (3H, s, OC$\underline{H}_3$); δ 6.69 (2H, d, $^3J = 8.8$ Hz, 3′-H 5′-H); δ 6.87 (1H ,d, $^3J = 8.2$ Hz, 5-H); δ 7.25 (1H, dd, $^3J = 8.1$ Hz, $^4J = 2.2$ Hz, 6-H); δ 7.42 (1H, d, $^3J = 8.0$ Hz, 7-H); δ 7.92 (2H, d, $^3J = 8.8$ Hz, 2′-H 6′-H). Accurate MS ES$^+$ *m/z* $[M+H]^+$ 257.0730 (calculated for $C_{14}H_{13}N_2OS$ 257.0743). Mp: 142.5–143 °C.

*4.2.1.5. 4-Hydroxy-2-(4′-aminophenyl)-1,3-benzothiazole (**5a**), method D.* A dispersion of **4a** (3.85 g, 15 mmol) in dichloromethane (180 ml) was cooled to −70 °C under nitrogen. Over a period of 1 h, 36 mmol BBr_3 (36 ml of a 1 M solution in dichloromethane) was added slowly, after which the mixture was stirred for another hour at −70 °C. The suspension was allowed to warm up to RT and was stirred for 12 h. The suspension was cooled to −70 °C and methanol was added slowly until no more gas evolved. After warming up to RT, 2 M sodium hydroxide (400 ml) was added. The aqueous layer was separated and neutralized with 3 M hydrochloric acid. The precipitate was filtered off and dried in a vacuum oven to yield 3.4 g of **5a** (14 mmol, 93%) as a brown powder. ^{1}H NMR ($CDCl_3$, 200 MHz): δ 6.67 (2H, d, $^3J = 8.4$ Hz, 3′-H 5′-H); δ 6.84 (1H, d, $^3J = 8.0$ Hz, 5-H); δ 7.15 (1H, dd, $^3J = 7.9$ Hz, 6-H); δ 7.39 (1H, d, $^3J = 7.6$ Hz, 7-H); δ 7.74 (2H, d, $^3J = 8.4$ Hz, 2′-H 6′-H); δ 9.93 (1H, s, O$\underline{H}$). Accurate MS ES$^+$ *m/z* $[M+H]^+$ 243.0599 (calculated for $C_{13}H_{11}N_2OS$ 243.0587). Mp: 210–212 °C.

4.2.2. Synthesis of 5-hydroxy-2-(4′-aminophenyl)-1,3-benzothiazole (**5b**)

4.2.2.1. N-*(2′-Chloro-5′-methoxyphenyl)-4-nitrobenzamide (**1b**).* Compound **1b** was synthesized following method A starting from 6-chloro-*m*-anisidine hydrochloride (10 g, 52 mmol) and *p*-nitrobenzoyl chloride (9.75 g, 52 mmol) in pyridine (50 ml). This yielded 12.28 g of **1b** (40 mmol, 77% yield). ^{1}H NMR (DMSO-d_6, 200 MHz): δ 3.85 (3H, s, OC$\underline{H}_3$); δ 6.70 (1H, dd, $^3J = 7.5$ Hz, 4′-H); δ 7.31 (1H, d, $^3J = 8.4$ Hz, 3′-H); δ 8.07 (2H, d, $^3J = 8.4$ Hz, 2-H 6-H); δ 8.21 (1H, d, $^3J = 8.8$ Hz, 6′-H); δ 8.38 (2H, d, $^3J = 7.6$ Hz, 3-H 5-H); δ 8.45 (1H, s, N$\underline{H}$-CO). Accurate MS ES$^+$ *m/z* $[M+H]^+$ 307.0480 (calculated for $C_{14}H_{11}ClN_2O_4$ 307.0469).

4.2.2.2. N-*(2′-Chloro-5′-methoxyphenyl)-4-nitrothiobenzamide (**2b**).* Compound **2b** was synthesized from **1b** (12.28 g, 40 mmol) following method B. A bright, orange solid was obtained (12 g, 37 mmol, 93%). ^{1}H NMR (DMSO-d_6, 200 MHz): δ 3.82 (3H, s, OC$\underline{H}_3$); δ 6.83 (1H, dd, $^3J = 7.4$ Hz, 4′-H); δ 7.38 (1H, d, $^3J = 7.8$ Hz, 3′-H); δ 7.97 (2H, d, $^3J = 7.4$ Hz, 2-H 6-H); δ 8.28 (2H, d, $^3J = 8.4$ Hz, 3-H 5-H); δ 8.51 (1H, s, 6'-H); δ 9.4 (1H, s, N$\underline{H}$-CS). Accurate MS ES$^+$ *m/z* $[M+H]^+$ 323.0252 (calculated for $C_{14}H_{11}ClN_2O_3S$ 323.0240). Mp: 136.2–138.2 °C.

*4.2.2.3. 5-Methoxy-2-(4′-nitrophenyl)-1,3-benzothiazole (**3b**), method E.* Sodium (368 mg, 16 mmol) was dissolved in methanol (20 ml), the solvent was evaporated under reduced pressure and the residue was added to a solution of **2b** (3.23 g, 10 mmol) in *N*-methyl-2-pyrrolidone (NMP, 50 ml). The mixture was stirred overnight at

110 °C and then poured into water (200 ml). The precipitate was filtered off, dried under reduced pressure and purified using column chromatography with hexane/ethyl acetate (90:10 v/v) as eluent. This yielded 150 mg of **3b** (0.52 mmol, 5%). ^{1}H NMR ($CDCl_3$, 200 MHz): δ 3.91 (3H, s, OCH_3); δ 7.11 (1H, dd, $^3J = 9.0$ Hz, $^4J = 2.4$ Hz, 6-H); δ 7.58 (1H, d, $^4J = 2.2$ Hz, 4-H); δ 7.78 (1H, d, $^3J = 8.8$ Hz, 7-H); δ 8.21 (2H, d, $^3J = 8.8$ Hz, 2′-H 6′-H); δ 8.33 (2H, d, $^3J = 8.8$ Hz, 3′-H 5′-H). Accurate MS ES$^+$ m/z $[M+H]^+$ 287.0493 (calculated for $C_{14}H_{10}N_2O_3S$ 287.0485). Mp: 195–196 °C.

*4.2.2.4. 5-Methoxy-2-(4′-aminophenyl)-1,3-benzothiazole (**4b**).* Compound **4b** was synthesized from **3b** (115 mg, 0.4 mmol) following method C, yielding 77 mg of **4b** (0.3 mmol, 75%). ^{1}H NMR ($CDCl_3$, 200 MHz): δ 3.88 (3H, s, OCH_3); δ 6.72 (2H, d, $^3J = 8.6$ Hz, 3′-H 5′-H); δ 6.97 (1H, dd, $^3J = 8.9$ Hz, $^4J = 2.6$ Hz, 4-H); δ 7.50 (1H, d, $^4J = 2.6$ Hz, 3-H); δ 7.68 (1H, d, $^3J = 8.8$ Hz, 5-H); δ 7.87 (2H, d, $^3J = 8.4$ Hz, 2′-H 6′-H). Accurate MS ES$^+$ m/z $[M+H]^+$ 257.0725 (calculated for $C_{14}H_{12}N_2OS$ 257.0743). Mp: 108–109 °C.

*4.2.2.5. 5-Hydroxy-2-(4′-aminophenyl)-1,3-benzothiazole (**5b**).* Compound **5b** was synthesized from **4b** (77 mg, 0.3 mmol) following method D, yielding 55 mg of **5b** (0.23 mmol, 77%). ^{1}H NMR (DMSO-d_6, 200 MHz): δ 5.85 (2H, s, NH_2); δ 6.66 (2H, d, $^3J = 8.4$ Hz, 3′-H 5′-H); δ 6.85 (1H, dd, $^3J = 7.9$ Hz, 6-H); δ 7.25 (1H, d, $^3J = 8.0$ Hz, 4-H); δ 7.72 (1H, d, $^3J = 7.6$ Hz, 7-H); δ 7.75 (2H, d, $^3J = 8.4$ Hz, 2′-H 6′-H); δ 9.67 (1H, s, OH). Accurate MS ES$^+$ m/z $[M+H]^+$ 243.0569 (calculated for $C_{13}H_{10}N_2OS$ 243.0587). Mp: 250.5–252.4 °C.

*4.2.3. Synthesis of 7-hydroxy-2-(4′-aminophenyl)-1,3-benzothiazole (**5c**)*

*4.2.3.1. N-(2′-Bromo-3′-methoxyphenyl)-4-nitrobenzamide (**1c**).* Compound **1c** was synthesized following method A starting from 2-bromo-3-aminoanisole (5.05 g, 25 mmol) and *p*-nitrobenzoyl chloride (4.64 g, 25 mmol) in pyridine (100 ml). This yielded 5.02 g of **1c** (14.3 mmol, 57%). ^{1}H NMR (DMSO-d_6, 200 MHz): δ 3.89 (3H, s, OCH_3); δ 7.07 (1H, d, $^3J = 8.2$ Hz, 6′-H); δ 7.17 (1H, d, $^3J = 8.2$ Hz, 4′-H); δ 7.41 (1H, t, $^3J = 8.1$ Hz, 5′-H); δ 8.21 (2H, d, $^3J = 8.4$ Hz, 2-H 6-H); δ 8.39 (2H, d, $^3J = 8.8$ Hz, 3-H 5-H); δ 10.38 (1H, s, NH–CO). Accurate MS ES$^+$ m/z $[M+H]^+$ 352.9951 (calculated for $C_{14}H_{11}BrN_2O_4$ 352.9956). Mp: 242-243.6 °C.

*4.2.3.2. N-(2′-Bromo-3′-methoxyphenyl)-4-nitrothiobenzamide (**2c**).* Compound **2c** was synthesized from **1c** (4.56 g, 13 mmol) following method B, yielding 4.55 g of **2c** (12.4 mmol, 95%). ^{1}H NMR (DMSO-d_6, 200 MHz): δ 3.89 (3H, s, OCH_3); δ 7.07 (1H, d, $^3J = 8.0$ Hz, 6′-H); δ 7.13 (1H, d, $^3J = 8.0$ Hz, 4′-H); δ 7.40 (1H, t, $^3J = 5.4$ Hz, 5′-H); δ 8.21 (2H, d, $^3J = 8.8$ Hz, 2-H 6-H); δ 8.38 (2H, d, $^3J = 8.8$ Hz, 3-H 5-H); δ 10.37 (1H, s, NH-CS). Accurate MS ES$^+$ m/z $[M+H]^+$ 368.9739 (calculated for $C_{14}H_{11}BrN_2O_3S$ 368.9727). Mp: 174.5–176 °C.

*4.2.3.3. 7-Methoxy-2-(4′-nitrophenyl)-1,3-benzothiazole (**3c**).* Compound **3c** was synthesized from **2c** (4.04 g, 11 mmol) following method E, yielding 2.00 g of **3c** (7 mmol, 64%). ^{1}H NMR (DMSO-d_6, 200 MHz): δ 3.89 (3H, s, OCH_3); δ 7.15 (1H, d, $^3J = 8.4$ Hz, 6-H); δ 7.58 (1H, t, $^3J = 8.1$ Hz, 5-H); δ 7.77 (1H, d, $^3J = 7.8$ Hz, 4-H); δ 8.21 (2H, d, $^3J = 8.8$ Hz, 2′-H 6′-H); δ 8.39 (2H, d, $^3J = 5.1$ Hz, 3′-H 5′-H). Accurate MS ES$^+$ m/z $[M+H]^+$ 287.0506 (calculated for $C_{14}H_{10}N_2O_3S$ 287.0485). Mp: 199.9–201.3 °C.

*4.2.3.4. 7-Methoxy-2-(4′-aminophenyl)-1,3-benzothiazole (**4c**).* Compound **4c** was synthesized from **3c** (1.80 g, 6.3 mmol) following method C, yielding 1.12 g of a yellow solid (3.9 mmol, 62%). ^{1}H NMR ($CDCl_3$, 200 MHz): δ 3.90 (3H, s, OCH_3); δ 6.67 (2H, d, $^3J = 8.6$ Hz, 3′-H 5′-H); δ 6.77 (1H, d, $^3J = 8.0$ Hz, 6-H); δ 7.38 (1H, t, $^3J = 8.3$ Hz, 5-H); δ 7.63 (1H, d, $^3J = 8.0$ Hz, 4-H); δ 7.90 (2H, d, $^3J = 8.4$ Hz, 2′-H 6′-H). Accurate MS ES$^+$ m/z $[M+H]^+$ 257.0723 (calculated for $C_{14}H_{12}N_2OS$ 257.0743). Mp: 151.1–154 °C.

*4.2.3.5. 7-Hydroxy-2-(4′-aminophenyl)-1,3-benzothiazole (**5c**).* Compound **5c** was synthesized from **4c** (513 mg, 2 mmol) following method D. The product was purified using MPLC to yield 182 mg of **5c** (0.75 mmol, 38%). ^{1}H NMR (DMSO-d_6, 200 MHz): δ 6.67 (2H, d, $^3J = 8.4$ Hz, 3′-H 5′-H); δ 6.77 (1H, d, $^3J = 7.8$ Hz, 6-H); δ 7.26 (1H, t, $^3J = 7.7$ Hz, 5-H); δ 7.38 (1H, d, $^3J = 7.8$ Hz, 4-H); δ 7.75 (2H, d, $^3J = 8.0$ Hz, 2′-H 6′-H). Accurate MS ES$^+$ m/z $[M+H]^+$ 243.0581 (calculated for $C_{13}H_{10}N_2OS$ 243.0587). Mp: 253.2–255 °C.

*4.2.4. Synthesis of 4-hydroxy-2-(4′-methylaminophenyl)-1,3-benzothiazole (**6a**), method F*

A solution of **5a** (303 mg, 1.25 mmol) and methyl iodide (800 μl, 12 mmol) in 50 ml of acetonitrile was heated at 80 °C for 36 h. The organic solvent was removed under reduced pressure and the residue was purified using MPLC. This yielded 16 mg of **6a** (0.062 mmol, 5%). ^{1}H NMR ($CDCl_3$, 200 MHz): δ 3.01 (3H, s, CH_3); δ 6.64 (2H, d, $^3J = 8.8$ Hz, 3′-H 5′-H); δ 6.93 (1H, d, $^3J = 7.8$ Hz, 7-H); δ 7.21 (1H, dd, $^3J = 7.9$ Hz, $^4J = 3.0$ Hz, 6-H); δ 7.34 (1H, d, $^3J = 8.0$ Hz, 5-H); δ 7.89 (2H, d, $^3J = 8.8$ Hz, 2′-H 6′-H). Accurate MS ES$^+$ m/z $[M+H]^+$ 257.0753 (calculated for $C_{14}H_{11}N_2O_2S$ 257.0743). Mp: 193–195 °C.

*4.2.5. Synthesis of 5-hydroxy-2-(4′-methylaminophenyl)-1,3-benzothiazole (**6b**)*

*4.2.5.1. 2-Amino-4-methoxy-thiophenol (**7**).* To a mixture of ethylene glycol (23 ml) and 10 M sodium hydroxide (23 ml), 5-methoxy-2-methyl-benzothiazole (5 g, 28 mmol) was added and the mixture was refluxed for 2 h under nitrogen. After cooling to RT, the mixture was neutralized with concentrated hydrochloric acid and extracted with ethyl acetate (3 × 50 ml). The organic layer was dried on $MgSO_4$, filtered and evaporated to dryness under reduced pressure. The obtained product **7** was used without further purification.

*4.2.5.2. 5-Methoxy-2-(4′-methylaminophenyl)-1,3-benzothiazole (**8**).* A dispersion of **7** (2.4 g, 28 mmol) and 4-(methylamino)benzoic acid (2 g, 28 mmol) in polyphosphoric acid (PPA) (6 g) was stirred at 180 °C for 3 h. After cooling to RT, 10% (m/v) sodium carbonate solution (100 ml) was added and the water layer was extracted with ethyl acetate (2 × 100 ml). The combined organic fractions were washed with brine, dried on $MgSO_4$, filtered and evaporated to dryness under reduced pressure. Purification was done using column chromatography with hexane/ethyl acetate (80:20 v/v) as eluent. This yielded 81 mg of **8** (0.3 mmol, 1%). ^{1}H NMR (DMSO-d_6): δ 2.78 (3H, s, NCH_3); δ 3.73 (3H, s, OCH_3); δ 4.00 (1H, s, NH); δ 6.49 (2H, d, $^3J = 8.0$ Hz, 3′-H 5′-H); δ 7.06 (1H, d, $^3J = 7.8$ Hz, 6-H); δ 7.26 (2H, d, $^3J = 8.8$ Hz, 2′-H 6′-H); δ 7.74 (1H, s, 4-H); δ 8.01 (1H, d, $^3J = 7.8$ Hz, 7-H). Accurate MS ES$^+$ m/z $[M+H]^+$ 271.0900 (calculated for $C_{15}H_{14}N_2OS$ 271.0879).

*4.2.5.3. 5-Hydroxy-2-(4′-methylaminophenyl)-1,3-benzothiazole (**6b**).* Compound **6b** was synthesized from **8** (70 mg, 0.26 mmol) following method D, yielding 45 mg of **6b** (0.18 mmol, 69%). ^{1}H NMR (DMSO-d_6): δ 2.75 (3H, s, CH_3); δ 6.40 (1H, s, NH); δ 6.63 (2H, d, $^3J = 8.8$ Hz, 2′-H 6′-H); δ 6.84 (1H, d, $^3J = 7.8$ Hz, 6-H); δ 7.25 (1H, s, 4-H); δ 7.73 (1H, d, $^3J = 7.8$ Hz, 7-H); δ 7.77 (2H, d, $^3J = 8.0$ Hz, 3′-H 5′-H); δ 9.64 (1H, s, OH). Accurate MS ES$^+$ m/z $[M+H]^+$ 257.0743 (calculated for $C_{14}H_{12}N_2OS$ 257.0743). Mp: 260–261 °C.

*4.2.6. Synthesis of 7-hydroxy-2-(4′-methylaminophenyl)-1,3-benzothiazole (**6c**)*

Compound **6c** was synthesized from **5c** (30 mg, 0.12 mmol) following method F, yielding 5.7 mg of **6c** (0.022 mmol, 18% yield).

^{1}H NMR (DMSO-d_6): δ 2.51 (3H, s, C$\underline{H}_3$); δ 5.80 (1H, s, N$\underline{H}$); δ 6.64 (2H, d, ^3J = 10.9 Hz, 3′-H 5′-H); δ 6.76 (1$\underline{H}$, d, ^3J = 9.3 Hz, 6-$\underline{H}$); δ 7.26 (1H, t, ^3J = 7.0 Hz, 5-H); δ 7.38 (2H, d, ^3J = 6.2 Hz, 2′-H 6′-H); δ 7.80 (1H, d, ^3J = 10.9 Hz, 4-H); δ 9.30 (1H, s, O$\underline{H}$). Accurate MS ES$^+$ m/z [M + H]$^+$ 257.0722 (calculated for $C_{14}H_{12}N_2OS$ 257.0743). Mp: 245–245.8 °C.

4.3. Radiolabelling

4.3.1. Synthesis of 4-hydroxy-2-(4′-[^{11}C]methylaminophenyl)-1,3-benzothiazole ([^{11}C]**6a**), 5-hydroxy-2-(4′-[^{11}C]methylaminophenyl)-1,3-benzothiazole ([^{11}C]**6b**) and 7-hydroxy-2-(4′-[^{11}C]methylaminophenyl)-1,3-benzothiazole ([^{11}C]**6c**)

With a stream of He, [^{11}C]$CH_3OSO_2CF_3$ [25] was bubbled through 0.3 ml of a solution of **5a** (3 mg/ml in anhydrous acetonitrile) at RT for 30 s. The reaction mixture was diluted with 5 ml of water and passed over an activated Sep-Pak® light C18 cartridge (Waters). The cartridge was rinsed with 5 ml of water and [^{11}C]**6a** was eluted from the cartridge with 0.75 ml of methanol, after which the eluate was applied on an Econosphere C18 column (250 mm × 10 mm; 10 μm, Alltech) which was eluted with an isocratic mixture of 0.05 M ammonium acetate/acetonitrile (50:50 v/v) at a flow rate of 3 ml/min. The peak containing [^{11}C]**6a** was identified using radiometric and UV detection (254 nm), and isolated. For the synthesis of [^{11}C]**6b** and [^{11}C]**6c**, 0.5 ml of a solution (1 mg/ml in acetone) of **5b** or **5c**, respectively, was used.

4.4. Partition coefficient

The lipophilicity of the RP-HPLC isolated ^{11}C-complexes was determined using a modification of the method described by Yamauchi and coworkers [26]. To a test tube containing 2 ml of 1-octanol and 2 ml of 0.025 M phosphate buffer pH 7.4, 25 μl of the RP-HPLC isolated ^{11}C-complex was added. The test tube was vortexed at room temperature for 3 min followed by centrifugation at 2700 g for 10 min. Aliquots of 60 μl and 500 μl were drawn from the 1-octanol and buffer phases, respectively, and weighed. The radioactivity in each aliquot was counted using a gamma counter and the partition coefficient P was calculated using the following equation:

$$P = \frac{\text{cpm/ml octanol}}{\text{cpm/ml buffer}} \text{ with cpm} = \text{counts per minute}$$

Experiments were performed in triplicate.

4.5. Determination of the affinity of the authentic non-radiolabelled derivatives for post-mortem human AD brain homogenates

4.5.1. Preparation of brain tissue homogenates

Post-mortem brain tissues were obtained from four AD patients and four age-matched control persons at autopsy, and neuropathological diagnosis was confirmed by current criteria (NIA-Reagan Institute Consensus Group, 1997). The cerebellum and the affected temporal or parietal cortex of AD patients together with the corresponding regions from control persons were isolated. Gray matter was carefully separated from white matter from the cortical tissues. Homogenates were then prepared in phosphate buffered saline (PBS, pH 7.4) at a concentration of approximately 100 mg wet tissue/ml (motor-driven glass homogenizer with setting of 6 for 30 s). The homogenates were aliquoted into 1-ml portions and stored at −70 °C for 3–6 months without loss of binding signal.

4.5.2. Binding studies

Binding assays were carried out according to a method described previously [27] using [^{125}I]IMPY (6-iodo-2-(4′-dimethylamino)phenyl-imidazo[1,2]pyridine) with a specific activity of 81.4 TBq/mmol and more than 95% radiochemical purity [16]. Binding assays were carried out in 12 mm × 75 mm borosilicate glass tubes. For saturation studies, the reaction mixture contained 50 μl of post-mortem AD brain homogenate (20–50 μg), 50 μl of a [^{125}I]IMPY solution in PBS (0.02–0.04 nM) and 40 μl of a solution of the test compound (**6a**, **6b** and **6c**; 10^{-7}–10^{-10} M diluted serially in PBS containing 0.1% bovine serum albumin) in a final volume of 1 ml. Non-specific binding was defined in the presence of 600 nM non-radioactive IMPY in the same assay tubes. For the competition binding studies, concentrations of 10^{-5}–10^{-10} M of the compounds and 0.06 nM [^{125}I]IMPY were used. The mixtures were incubated at 37 °C for 2 h, and the bound and the free radioactivity were separated by vacuum filtration through Whatman GF/B filters using a Brandel M-24R cell harvester (London, England) followed by two 3-ml washes with PBS at room temperature. Filters containing the bound iodine-125 ligand were counted in a gamma counter (Packard 5000, Ramsey, Minnesota, USA) with 70% counting efficiency. Under the assay conditions, the specifically bound fraction was less than 15% of the total radioactivity. Protein determinations were performed with Lowry's method [28] using bovine serum albumin as a standard. The results of saturation and inhibition experiments were subjected to non-linear regression analysis using EBDA by which K_d and K_i values were calculated.

4.6. Binding to amyloid plaques in mouse and human AD brain sections

4.6.1. Paraffin sections

Transgenic mice overexpressing human amyloid precursor protein (APP) (London mutation [29]) were anaesthetized with Nembutal® (pentobarbital, intraperitoneal injection, 2 μl/g) and the brain was flushed transcardially with ice-cold saline. The brain was removed and post-fixed overnight with 4% paraformaldehyde in PBS. One part of the brain was stored in 0.1% sodium azide in PBS at 4 °C. The other part was processed for paraffin embedding. Sagittal sections (8 μm) were cut using a Microm HM 340 E microtome (Microm, Walldorf, Germany). Prior to incubation, paraffin sections were taken through two 5-min washes with xylol, followed by 1-min sequential washes with 100%, 100%, 90%, 70%, 50% ethanol and PBS. After rehydration, the sections were incubated for 1 h with one of the cold compounds (**6a**, **6b** or **6c**) at a concentration of 1 μM. After 1 h, the brain sections were rinsed with tap water and coverslipped with Mowiol-DABCO. For the preparation of the Mowiol-DABCO mixture, 10 g of Mowiol (Calbiochem, Darmstadt, Germany) and 90 ml of PBS pH 7.4 was stirred for 4–6 h, then 3.25 g DABCO (1,4 diazabicyclo[2.2.2]octane; Sigma–Aldrich) was added followed by 40 ml of glycerin and the mixture was stirred overnight. The mixture was centrifuged at 15 000 rpm for 30 min, aliquoted and stored at −20 °C. The aliquots were thawed before use and can be refrozen after use. For immunohistochemical staining, the same deparaffinization protocol was used. The sections were boiled for 10 min in a microwave (Miele M 326 G) with 0.01 M citrate buffer pH 6 as antigen retrieval. After cooling down for 20 min the sections were rinsed with PBS followed by treating them with 1.5% H_2O_2 in PBS/methanol (50:50 v/v) to inhibit endogenous peroxidase. Non-specific binding was blocked by treatment with PBS containing 0.05% Tween® 20 (PBST) and 10% fetal calf serum (FCS). The sections were incubated overnight with pan β-amyloid (AB-1) polyclonal antibodies (Oncogene Research Products, San Diego, CA, U.S.A.) diluted 1/1000 in PBST 10% FCS at 4 °C for compound **6a**. For compounds **6b** and **6c**, the sections were incubated overnight with AβN25 monoclonal antibody, diluted 1/500 in PBST with 10% FCS at 4 °C. After rinsing in PBST, the sections were incubated for 1 h with 1/500 diluted goat anti-mouse biotin (goat anti-rabbit for pan Aβ) (Vector Laboratories, Burlingame, CA, U.S.A.) in PBST with 10% FCS. Then sections were incubated with Avidin Biotin Complex

(Vectastain Elite ABC-peroxidase kit, Vector Laboratories) dissolved in PBST with 10% FCS for 30 min at room temperature. Peroxidase activity was developed with 3,3′-diaminobenzidine, after which the sections were counterstained with haematoxylin. Paraffin embedded human AD brain was stained following the same procedure as described for mouse brain. AD brain was treated according to the regulations of the Ethical Committee of the hospital.

4.6.2. Vibratome sections

For vibratome sections, the paraformaldehyde-fixed brain was cut into sagittal sections of 40 μm thickness with a Microm HM 650 V vibration microtome (Microm). The sections were incubated for 1 h at room temperature with one of the cold compounds (**6a**, **6b** or **6c**) at a concentration of 1 μM. After incubation, the sections were rinsed for 5 s in tap water and coverslipped using a Mowiol-DABCO solution. Immunohistochemical staining of vibratome sections was performed using the same protocol as described for paraffin sections with some modifications. No microwave pretreatment was performed and the solution containing 0.05% Tween® 20 in PBS buffer was replaced by a 0.1% Triton X100 solution. The dilution of the pan β-amyloid antibody was 1/5000 for compound **6a**. For compounds **6b** and **6c**, the dilution of the AβN25 antibody was 1/2000. After rinsing in PBST, the sections were incubated for 1 h with 1/500 diluted goat anti-mouse horseradish peroxidase (Dako A/S, Denmark) in PBST with 10% FCS. Peroxidase activity was developed with 3,3′-diaminobenzidine. After washing with PBS, the sections were mounted on silane-coated glasses and after drying they were counterstained with haematoxylin, the sections were dehydrated by passage through a graded series of alcohol and xylol and coverslipped with DePeX mounting medium. Fluorescence microscopy was performed using a Leica DMR microscope equipped with a digital Leica DC480 camera and a UV filter set with the following specifications: excitation filter 355–425 nm; dichromatic mirror 455 nm; emission 470 nm longpass filter. The images were collected and processed with Leica IM500 image processing software (Heerbrugg, Switzerland).

4.7. Biological evaluation in mice

The RP-HPLC peak containing the desired labelled compound was isolated, concentrated by bubbling nitrogen-gas through it at 50 °C to evaporate the acetonitrile and diluted with saline to a concentration of 37 MBq/ml. Male NMRI mice ($n = 8$ per compound) were sedated with an intraperitoneal injection of 0.1 ml Hypnorm® (fentanyl citrate 63 μg/ml + fluanisone 2 mg/ml) and injected with the compound via a tail vein. The mice were sacrificed by decapitation at 2 or 60 min p.i. ($n = 4$ at each time point). Blood was collected in a tared tube and weighed. All organs and other body parts were dissected and weighed and their activity was counted using a gamma counter. Results were corrected for background activity and are expressed as percentage of the injected dose per organ (% ID) or as percentage of the injected dose per gram tissue (% ID/g). To calculate the activity in the blood, blood mass was assumed to be 7% of body mass.

Acknowledgments

The authors wish to acknowledge the help of Christelle Terwinghe (Radiopharmacy, UZLeuven, Leuven, Belgium) for performing the biodistribution studies.

References

[1] A.F. Jorm, D. Jolley, Neurology 51 (1998) 728–733.
[2] D.J. Selkoe, Phys. Rev. 81 (2001) 741–766.
[3] T.C. Gamblin, F. Cen, A. Zambrano, A. Abraha, S. Lagalwar, A.L. Guillozet, M. Lu, Y. Fu, F. Garcia-Sierra, N. LaPointe, R. Miller, R.W. Berry, L.I. Binder, V.L. Cryns, PNAS 100 (2003) 10032.
[4] M. Rapoport, H.N. Dawson, L.I. Binder, M.P. Vitek, A. Ferreira, Proc. Natl. Acad. Sci. U.S.A. 99 (2002) 6364–6369.
[5] K.B. Rank, A.M. Pauley, K. Bhattacharya, Z. Wang, D.B. Evans, T.J. Fleck, J.A. Johnston, S.K. Sharma, FEBS Lett. 514 (2002) 263–268.
[6] J.A. Hardy, G.A. Higgins, Science 256 (1991) 184–185.
[7] R.C. Young, R.C. Mitchell, R.H. Brown, C.R. Ganellin, R. Griffiths, M. Jones, K.K. Rana, D. Saunders, I.R. Smith, N.E. Sore, T.J. Wilks, J. Med. Chem. 31 (1988) 656–671.
[8] D.D. Dischino, M.J. Welch, M.R. Kilbourn, M.E. Raichle, J. Nucl. Med. 24 (1983) 1030–1038.
[9] W.E. Klunk, M.L. Debnath, J.W. Pettegrew, Neurobiol. Aging 15 (1994) 691–698.
[10] Z.P. Zhuang, W.E. Klunk, J. Wang, G.F. Huang, M.L. Debnath, D.P. Holt, C.A. Mathis, J. Med. Chem. 44 (2001) 1905–1914.
[11] M. Ono, A. Wilson, J. Nobrega, D. Westaway, P. Verhoeff, Z.P. Zhuang, M.P. Kung, H.F. Kung, Nucl. Med. Biol. 30 (2003) 565–571.
[12] E. Agdeppa, V. Kepe, J. Liu, M. Flores-Torres, N. Satyamurthy, A. Petric, G. Cole, G. Small, S.C. Huang, J. Barrio, J. Neurosci. 21 (2001) 1–5.
[13] W.E. Klunk, Y. Wang, G. Huang, M.L. Debnath, D.P. Holt, C.A. Mathis, Life Sci. 69 (2001) 1471–1484.
[14] W.E. Klunk, H. Engler, A. Nordberg, Y. Wang, G. Blomqvist, D. Holt, M. Bergström, I. Savitcheva, G. Huang, S. Estrada, B. Ausén, M. Debnath, J. Barletta, J. Proce, J. Sandell, B. Lopresti, A. Wall, P. Koivisto, G. Antoni, C. Mathis, B. Langström, Ann. Neurol. 55 (2004) 306–319.
[15] H. Archer, P. Edison, D. Brooks, J. Barnes, C. Frost, T. Yeatman, N. Fox, M. Rossor, Ann. Neurol. 60 (2006) 145–147.
[16] Z.P. Zhuang, M.P. Kung, C. Hou, K. Plossel, D. Skovronsky, T.L. Gur, J.Q. Trojanowski, V. Lee, H.F. Kung, Nucl. Med. Biol. 28 (2001) 887–894.
[17] Z.P. Zhuang, M.P. Kung, A. Wilson, C.W. Lee, K. Plössl, C. Hou, D. Holtzman, H.F. Kung, J. Med. Chem. 46 (2003) 237–243.
[18] T. Suemoto, N. Okamura, T. Shiomitsu, M. Suzuki, H. Shimadzu, H. Akatsu, T. Yamamoto, Y. Kudo, T. Sawada, Neurosci. Res. 48 (2004) 65–74.
[19] C. Rowe, U. Ackerman, W. Browne, R. Mulligan, K. Pike, G. O'Keefe, H. Tochon-Danguy, G. Chan, S. Berlangieri, G. Jones, K. Dickinson-Rowe, H. Kung, W. Zhang, M. Kung, D. Skovronsky, T. Dyrks, G. Holl, S. Krause, M. Friebe, L. Lehman, S. Lindermann, L. Dinkelborg, C. Masters, V. Villemagne, Lancet Neurol. 7 (2008) 129–135.
[20] D.-F. Shi, T.D. Bradshaw, S. Wrigley, C.J. McCall, P. Lelieveld, I. Fichtner, M.F.G. Stevens, J. Med. Chem. 39 (1996) 3375–3384.
[21] I. Hutchinson, M.F.G. Stevens, A.D. Westwell, Tetrahedron Lett. 41 (2000) 425–428.
[22] M.E. Krolski, A.F. Renaldo, D.E. Rudisill, J.K. Stille, J. Org. Chem. 53 (1988) 1170–1176.
[23] A.J. Lin, S. Kasina, J. Heterocycl. Chem. 18 (1981) 759–761.
[24] N. Okamura, T. Suemoto, H. Shimadzu, M. Suzuki, T. Shiomitsu, H. Akatsu, T. Yamamoto, M. Staufenbiel, K. Yanai, H. Arai, H. Sasaki, Y. Kudo, T. Sawada, J. Neurosci. 24 (2004) 2535–2541.
[25] D.M. Jewett, Appl. Radiat. Isot. 43 (1992) 1383–1385.
[26] H. Yamauchi, J. Takahashi, S. Seri, H. Kawashima, H. Koike, M. Kato-Azuma, in: M. Nicolini, G. Bandoli, U. Mazzi (Eds.), Technetium and Rhenium in Chemistry and Nuclear Medicine, vol. 3, Cortina International, Verona, Italy, 1989, pp. 475–502.
[27] M.P. Kung, C. Hou, Z.P. Zhuang, D. Skovronsky, H.F. Kung, Brain Res. 1025 (2004) 89–105.
[28] P.J. Munson, D. Rodbard, Anal. Biochem. 107 (1980) 220–239.
[29] F. van Leuven, Prog. Neurobiol. 61 (2000) 305–312.